RSC Advances

This is an *Accepted Manuscript*, which has been through the Royal Society of Chemistry peer review process and has been accepted for publication.

Accepted Manuscripts are published online shortly after acceptance, before technical editing, formatting and proof reading. Using this free service, authors can make their results available to the community, in citable form, before we publish the edited article. This *Accepted Manuscript* will be replaced by the edited, formatted and paginated article as soon as this is available.

You can find more information about *Accepted Manuscripts* in the Information for Authors.

Please note that technical editing may introduce minor changes to the text and/or graphics, which may alter content. The journal's standard Terms & Conditions and the Ethical guidelines still apply. In no event shall the Royal Society of Chemistry be held responsible for any errors or omissions in this *Accepted Manuscript* or any consequences arising from the use of any information it contains.

ROYAL SOCIETY OF CHEMISTRY

www.rsc.org/advances

Effects of silicon dioxide surface roughness on Raman characteristics and mechanical properties of graphene

Quan Wang[1,2], Yun Li[1]，Bing Bai[1],Wei Mao[1], Zegao Wang[3], Naifei Ren[1]

1. School of Mechanical engineering, Jiangsu University, Zhenjiang 212013, P.R.China

2. State Key Laboratory of Transducer Technology, Chinese Academy of Sciences, Shanghai 200050, P.R.China

3. State Key Laboratory of Electronic Thin Films and Integrated Devices, University of Electronic Science and Technology of China, Chengdu 610054, P.R.China

The effects of the surface roughness of a silicon dioxide substrate on the mechanical properties and Raman scattering of graphene prepared by chemical vapor deposition were investigated.

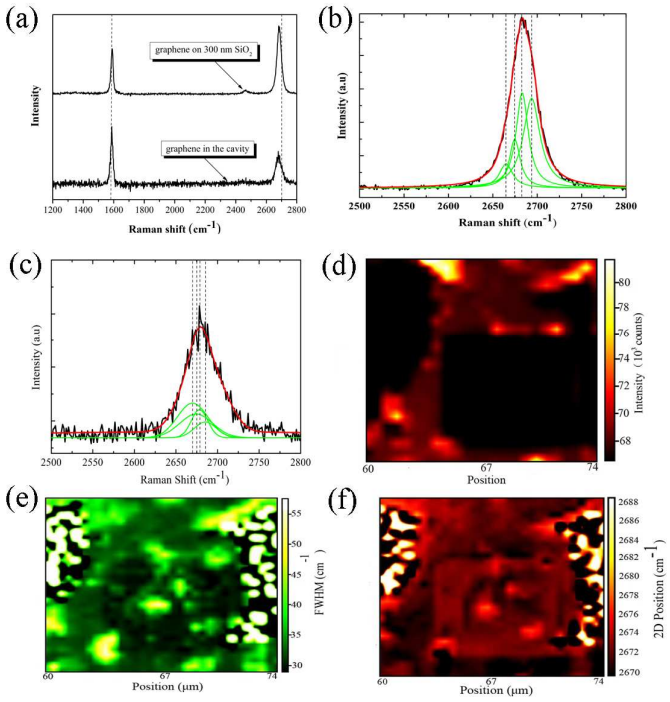

RSC Advances Accepted Manuscript

Effects of silicon dioxide surface roughness on Raman characteristics and mechanical properties of graphene

Quan Wang[1,2 a], Yun Li[1]， Bing Bai[1],Wei Mao[1], Zegao Wang[3], Naifei Ren[1]

1. School of Mechanical engineering, Jiangsu University, Zhenjiang 212013, P.R.China

2. State Key Laboratory of Transducer Technology, Chinese Academy of Sciences, Shanghai 200050, P.R.China

3. State Key Laboratory of Electronic Thin Films and Integrated Devices, University of Electronic Science and Technology of China, Chengdu 610054, P.R.China

RSC Advances Accepted Manuscript

Abstract

The effects of the surface roughness of a silicon dioxide substrate on the mechanical properties and Raman scattering of graphene prepared by chemical vapor deposition were investigated. Analysis of the Raman spectra of the graphene indicated that the strain induced on areas with different surface roughness was the main cause of a shift in the 2D band. Phonon scattering decreased the phonon velocity and the full width at half-maximum of the 2D band. Owing to the greater surface roughness, the shear stress was much greater at the interface between the graphene and the substrate than in other areas. These results provide a method of enhancing the interfacial strength to avoid device instability.

Keywords: Graphene; Silicon dioxide; Raman scattering; Surface roughness

[a] Author to whom correspondence should be addressed. Electronic mail: wangq@mail.ujs.edu.cn

1 Introduction

Graphene has attracted considerable scientific and technological interest since its discovery in 2004 [1, 2] owing to its unique properties, such as high carrier mobility [3] and intrinsic strength [4-6]. Because of these unusual properties, tantalizing potential applications of graphene, ranging from field effect transistors to chemical and biochemical sensors, have emerged [7-9]. However, to realize practical graphene devices, many problems must be solved, such as band gap control, morphology control, and interfacial engineering between graphene and the substrate.

The properties of graphene are very sensitive to the environment; for instance, a supporting substrate causes adsorption on the surface of graphene [10]. These effects have been reported, but the interface structure between graphene and the substrate surface is not yet well understood. A recent theoretical study by Gao *et al* [11, 12] reported the van der Waals (vdW) force between graphene and its substrate. It predicted that the adhesion energy depends sensitively on the morphology, which in turn depends on both the surface roughness and bending modulus of graphene. However, the factors influencing the surface roughness of graphene are unclear. Recent experiments using a combined scanning electron microscopy/atomic force microscopy/scanning tunneling microscopy (SEM/AFM/STM) technique indicated that the graphene partially conforms to the underlying SiO_2 substrate and is 60% smoother than the SiO_2 surface [13]. It was further revealed that graphene and few-layer graphene partially follow the surface morphology of various substrates (e.g., GaAs, InGaAs, and SiO2) [14]. Xiong and Gao discovered that the corrugation of graphene on the substrate is not affected by the surface amplitude but increases as the surface wavelength increases [15]. Researchers have also examined the effects of the substrate roughness. However, few studies have focused on the effects of the substrate surface roughness on the mechanical properties and Raman scattering of graphene.

RSC Advances Accepted Manuscript

Raman spectroscopy (RS) has proven to be a key diagnostic tool for identifying the number of graphene layers and obtaining their physical properties [16]. Researchers have recently published works regarding RS studies of the mechanical strain. Jie *et al.* presented in-situ and real-time Raman spectra of graphene under controllable biaxial conditions in a graphene/lead magnesium niobate–lead titanate hybrid system, which imposed compressive biaxial strain on the graphene, resulting in a blue shift in the 2D band [17]. Previous studies demonstrated that variations in the Raman 2D band of graphene can serve as a spectroscopic fingerprint for detecting induced strain in graphene [18, 19]. In addition, the high sensitivity of the 2D peak frequency ω_{2D} to the phonon velocity v_{TO} will influence the Raman spectral features with even a slight change in the structure of graphene due to the vdW interaction.

In this study, we demonstrate the effects of the surface roughness of substrates obtained by various methods on the properties of graphene, such as the shear stress, tensile strain, and Raman scattering obtained using RS and AFM.

2 Experiments

First, 300-nm-thick silicon dioxide was formed on a highly n-doped silicon substrate by thermal oxidation at 1000 ℃. Reactive-ion etching was employed to form holes using lithography to obtain flat and patterned substrates. Fig. 1a present the SEM image of the substrate. Finally, the graphene was transferred to the substrate as shown in Fig. 1. The Au/TiW electrode shown in Fig.1c is for the further study of graphene-based field effect transistor. The graphene samples were prepared by chemical vapor deposition on the copper substrate as in previous research. The graphene grown on Cu foils was deposited onto SiO_2/Si substrates of different

RSC Advances Accepted Manuscript

thicknesses using the standard transfer method [20].

AFM was employed to measure the morphology and surface roughness of the graphene samples. The measurements were performed in tapping mode to avoid damaging or modifying the graphene.

3 Results and discussion

Fig. 1(b) presents an AFM micrograph of a sample, showing that the cavity and the 300-nm-thick SiO_2 layer are both covered with graphene (C-graphene and S-graphene, respectively). Fig. 1(b) also shows that the transfer process generated wrinkles, folds, and cracks in the graphene, which also appear in Figs. 1(c) and 1(d). In Fig. 1(c), we cannot distinguish the graphene covering the cavity because its high light transmittance produces a lower contrast ratio with the substrate [21]. Consequently, SEM was used to demonstrate that the graphene was pulled into the cavity rather than suspended on it.

The morphologies of the cavity and the 300-nm-thick SiO_2 layer are considered in order to understand the differences between S-graphene and C-graphene. The morphologies can be characterized according to the surface roughness. The average roughness parameter R_a is used to denote the surface roughness, which is defined as

$$R_a = \frac{1}{L}\int_0^L |Z| dx, \quad (1)$$

where Z is the height of the surface relative to the baseline, and L is the length of the sample [22]. The results for the surface roughness and surface morphology are shown in Figs. 2 and 3, respectively. In Figs. 2(b) and (d), the surface roughness of the cavity

RSC Advances Accepted Manuscript

according to Equation (1) is larger than that of the 300-nm-thick SiO_2 layer, which corresponds to the 3D morphology of the structure, as shown in Fig. 3.

We also investigated the Raman spectra of graphene covering flat and patterned substrates to investigate the effects of the substrate surface roughness on the interfacial force, strain, and Raman scattering under ambient conditions. The Raman information for the graphene was obtained using a micro-Raman spectrometer (Horiba Jobin-Yvon) with a spectral resolution of ~1 cm^{-1} and an excitation laser with a wavelength of 532 nm. The power on the sample was maintained at less than 2 mW to avoid damaging or heating the graphene. Fig. 4(a) presents Raman spectra obtained from the S-graphene and C-graphene in Fig. 1(c). The spectrum of the S-graphene shows two prominent Raman peaks-G and 2D-located at ~1588 cm^{-1} and ~2683 cm^{-1}, respectively, indicating substantial p-type charge doping. Another asymmetric peak called the D+D′′ mode is observed near 2450 cm^{-1}, indicating a two-phonon process involving the contributions of a transverse optical (TO) and longitudinal acoustic (LA) phonon [23]. The G and 2D peaks are also prominent in C-graphene, and their special features are shown in greater detail in the Raman spectrum of C-graphene than in that of S-graphene. The G peak frequency for C-graphene is ~1 cm^{-1} lower than that for S-graphene; this difference is negligible, which may demonstrate that the degree of charge doping in C-graphene and S-graphene is equal. The 2D peak of C-graphene located at ~2678 cm^{-1}, which is ~5 cm^{-1} lower than that of S-graphene. In addition, the full width at half-maximum (FWHM) values for C-graphene and S-graphene are 36 cm^{-1} and 27 cm^{-1}, respectively. One notable difference between the two types of

RSC Advances Accepted Manuscript

graphene is that D+D″ is absent in C-graphene. As shown in Figs. 4(b) and 4(c), the 2D bands of S-graphene and C-graphene are fitted by Lorentz fitting and divided into four peaks.

To discuss the difference between S-graphene and C-graphene in detail, we present the maps of the G peak intensity (I_G), 2D FWHM, and 2D peak frequency (ω_{2D}) in Figs. 4(e), 4(f), and 4(g), respectively. In Fig. 4(a), we see that the 2D peak frequency of C-graphene is distributed in a range between ~2674 cm^{-1} and ~2680 cm^{-1}. However, the frequency of S-graphene is much higher than that of C-graphene, which is consistent with the results of point Raman measurements. The difference between the FWHM of the 2D peaks of S-graphene and C-graphene varies with the 2D peak frequency. The FWHM of C-graphene is smaller than that of S-graphene. In addition, the intensity of the G-band in C-graphene is moderately lower than that in S-graphene, as shown in Fig. 4(e).

The difference in surface roughness between the 300-nm-thick SiO_2 layer and the cavity is attributed to the difference in nanoparticle distribution. The intensity of scattering is related to the number of atomics (nanoparticles) distributed on the surface: more atomics produce a higher intensity of scattering. In Figs. 4(a) and 4(e), the intensities of the G band and the 2D band in the Raman spectra differ. The film's surface condition is responsible for the Raman scattering of graphene. According to the equation proposed by Basko [24],

$$\frac{dI_{2D}(\omega)}{d(\omega)} \propto \left[(\omega - \omega_{2D})^2 + \frac{\Gamma_{2D}^2}{4\left(2^{2/3} - 1\right)} \right]^{-3/2}, \qquad (2)$$

RSC Advances Accepted Manuscript

where ω_{2D} and Γ_{2D} denote the central frequency and FWHM of the 2D band, respectively. The linewidth of the 2D band feature (i.e., the FWHM) is expected to be given by

$$\Gamma_{2D} = 4\sqrt{2^{2/3}-1}\frac{\nu_{TO}}{\nu_F}\gamma_{eh}, \quad (3)$$

where $\nu_{TO}(\nu_F)$ is the phonon (Fermi) velocity, defined as the slope of the photonic (electronic) dispersion at the phonon (electron) momentum corresponding to a given laser energy, and γ_{eh} is the electronic broadening parameter. As indicated by Equations (2) and (3), the factor $\frac{\nu_{TO}}{\nu_F}$ plays an important role in determining the linewidth (FWHM) of the 2D band when γ_{eh} is constant. As discussed above, the G band of the Raman spectrum shifts slightly; in particular, E_F (the Fermi level) changes slightly, which can be ignored. Because it is defined as

$$\nu_F = \sqrt{\frac{2E_F}{m_e}}, \quad (4)$$

ν_F can be regarded as a constant. Therefore, ν_{TO} is responsible for the change in the linewidth. Because the solid is not a prefect vacuum, the phonon can be scattered naturally by the crystal lattice and defects originating in the solid, and the particles can be scattered from each other. The surface roughness of the cavity is greater than that of the 300-nm-thick SiO_2 layer. The scattering process of the phonon in the cavity is quite active compared with that in the SiO_2 layer. These phenomena cause the phonon velocity to decrease. Therefore, the FWHM of graphene in the flat area is higher than that in the cavity.

Raman mapping, as shown in Fig. 4(g), reveals a significant shift in the 2D peak

RSC Advances Accepted Manuscript

depending on the distribution of the local strain in the graphene. Therefore, it is desirable to investigate the difference in strain between S-graphene and C-graphene. The red line in Fig. 5 shows the 2D peak frequency along the position. The 2D peak frequency of the graphene covering the cavity is much lower than that of S-graphene. However, the 2D peak frequency of the graphene on the 300-nm-thick SiO_2 layer varies somewhat. Using the formula proposed by Mohiuddin *et al*. [25], we can calculate the exerted strain according to the Raman peak position shift as follows:

$$\gamma = \frac{\Delta\omega}{2\omega_0(1 - \nu)\varepsilon}, \quad (5)$$

where γ is the Grüneisen parameter, $\Delta\omega$ is the Raman frequency shift with applied strain, ω_0 is the Raman frequency without applied strain (2700 cm^{-1}), ν is the Poisson ratio of the substrate material, and ε is the strain induced on the sample. In this work, for the Grüneisen parameter of the 2D band, we use a value of 2.7 derived using the shift in the Raman peak. The strain in the graphene is calculated using Equation (5); the results are indicated by the black line in Fig. 5. The strain in the graphene is tensile strain due to the 2D peak's blue shift from 2700 cm^{-1}. C-graphene experienced a tensile strain of 0.3 %~0.45 %, and the strain in S-graphene was 0.2 %~0.3 %.

Assuming that the shear stress at the interface between the graphene and the substrate is balanced by the variation in the strain, the shear stress (τ) can be estimated using Equation (6):

$$\frac{d\sigma}{dx} = -\frac{\tau}{Et}, \quad (6)$$

where σ is the strain in the graphene shown in Fig. 3, x is the distance along the

RSC Advances Accepted Manuscript

position, *E* is the Young's modulus of graphene, and *t* is the thickness of the graphene [26]. The slopes of the lines in Fig. 3, i.e., $d\sigma/dx$, are displayed in Fig. 6. The slopes of the line in the area of the 300-nm-thick SiO_2 layer remain stable, whereas they fluctuate greatly in the cavity area. Considering Equation (6) and Fig. 6, we deduce that C-graphene undergoes greater shear stress than S-graphene.

The inner stress induced by mismatch between films and substrates can increase the surface roughness. Inversely, the surface roughness of the substrate can cause stress in films. To analyze this concept simply, the thickness of the film is defined as

$$h(x) = h_o + q\cos\frac{2\pi x}{\lambda}, \quad (7)$$

where *q* is the distance to the baseline, and λ is the wavelength of the cycle. Under the conditions of $q << \lambda$ and the first-order approximation, the enhanced surface energy in one cycle can be defined as

$$\Delta W_S = \pi^2 \frac{\gamma q^2}{\lambda}. \quad (8)$$

On the other hand, the ascending surface energy is equal to the work done by the surface tension stress at constant temperature and pressure; i.e.,

$$E\varepsilon dA = \sigma dA = \Delta W_s = \pi^2 \frac{\gamma q^2}{\lambda}, \quad (9)$$

where - ε is the strain under the surface tension stress. According to Equation (9), when the Young's modulus of graphene is constant, the strain induced in the graphene is related to *q*: a larger q leads to greater strain. As mentioned previously, the surface roughness of the 300-nm-thick SiO_2 layer is smaller. To facilitate the analysis, the surface of roughness is regarded as *q*. Thus, compared with the strain in the

RSC Advances Accepted Manuscript

300-nm-thick SiO_2 layer, the strain distributed in the cavity is quite high, which is consistent with the blue shift of the 2D band in the Raman spectrum.

4 Conclusions

The effects of the surface roughness of SiO_2 on the mechanical properties and Raman scattering of graphene were presented. Raman features, particularly the peak frequency and FWHM of the 2D band, differed significantly depending on whether the graphene was placed on a 300-nm-thick SiO_2 layer or on a cavity. It is concluded that the peak shift of the 2D band was due to the strain induced by the difference in the surface roughness. The high surface roughness of SiO_2 compared with the cavity leads to a higher surface energy and greater strain induced by the tension stress of the surface. The phonon scattering process, which is affected by the surface roughness, is responsible for the reduced phonon velocity v_{TO}, which narrows the FWHM of the 2D band in the cavity. The shear stress at the interface between the graphene and the substrate is much greater in the cavity owing to the greater surface roughness. These results have important implications for graphene nano-devices fabricated on silicon oxidation layers with different thicknesses using various techniques, and they provide a method of enhancing the interfacial strength and thereby ensuring the stability of such devices.

ACKNOWLEDGMENTS

This work was supported by the National Natural Science Foundation of China (No. 51175238), the Industrial Supporting Plan of Zhenjiang City (No.GY2013011) and "Six talent peaks" of high level talent selection and training project of Jiangsu Province（No.2013-ZBZZ-031）, the Priority

RSC Advances Accepted Manuscript

Academic Program Development of Jiangsu Higher Education Institutions and Graduate Research and Innovation Projects in Jiangsu University (No.KYXX_0029). The authors would like to thank Rong Ding, from Taizhou Sunano New Energy Co., Ltd for his technical direction and support in Raman spectrometry.

REFERENCES

[1] K.S. Novoselov, A.K. Geim, S.V. Morozov, D. Jiang, Y. Zhang, S.V. Dubonos, I.V. Grigorieva, A.A. Firsov, Electric field effect in atomically thin carbon films, Science, 306(2004)666–699.

[2] A.K. Geim, K.S. Novoselov, The rise of graphene, Nat Mater, 6(2007)183–191.

[3] K.S. Novoselov, A.K. Geim, S.V. Morozov, D. Jiang, M.I. Katsnelson, I.V. Grigorieva, S.V. Dubonos, A.A. Firsov, Two-dimensional gas of massless Dirac fermions in graphene, Nature, 438(2005)197–200.

[4] C.G. Lee, X.D. Wei, J.W. Kysar, J. Hone, Measurement of the elastic properties and intrinsic strength of monolayer graphene, Science, 321(2008)385–388.

[5] D.B. Zhang, E. Akatyeva, T. Dumitrică, Bending ultrathin graphene at the margins of continuum mechanics，Phys Rev Lett, 106(2011) 255503.

[6] X. Lü, J. Wu, T. Lin, D. Wan, F. Huang, X. Xie, M. Jiang, Low-temperature rapid synthesis of high-quality pristine or boron-doped graphene via Wurtz-type reductive coupling reaction，J Mater Chem, 21(2011)10685-10689.

[7] X. Wang, L. Zhi, K. Mullen, Transparent, conductive graphene electrodes for dye-sensitized solar cells, Nano Lett, 8(2008)323–327.

[8] G. Eda, G. Fanchini, M. Chhowalla, Large-area ultrathin films of reduced graphene oxide as a transparent and flexible electronic material, Nat Nanotechnol, 3(2008)270–274.

[9] F. Schedin, A.K. Geim, S.V. Morozov, E.W. Hill, P. Blake, M.I. Katsnelson, K.S. Novoselov, Detection of individual gas molecules adsorbed on graphene, Nat Mater, 6(2007)652–655.

[10] K. Nagashio, T. Yamashita, T. Nishimura, K. Kita, A. Toriumi, Electrical transport properties

RSC Advances Accepted Manuscript

of graphene on SiO_2 with specific surface structures, J Appl Phys, 110(2011)024513.

[11] W. Gao, R. Huang, Effect of surface roughness on adhesion of graphene membranes, J Phys D: Appl Phys, 44(2011)452001.

[12] W. Gao, P. Xiao, G. Henkelman, K.M. Liechti, R. Huang, Interfacial adhesion between graphene and silicon dioxide by density functional theory with van der Waals corrections，J Phys D: Appl Phys, 47(2014)255301.

[13] M. Ishigami, J.H. Chen, W.G. Cullen, M.S. Fuhrer, E.D. Williams, Atomic structure of graphene on SiO_2, Nano Lett, 7(2011)1643–1648.

[14] U. Stoberl, U. Wurstbauer, W. Wegscheider, D. Weiss, J. Eroms, Morphology and flexibility of graphene and few-layer graphene on various substrates, Appl Phys Lett, 93(2008)051906.

[15] L.T. Xiong, Y.W. Gao, Surface roughness and size effects on the morphology of graphene on a substrate, Phys E (Amsterdam, Neth), 54(2013)78–85.

[16] W.Z. Bao, I. Calizo, F. Miao, C.N. Lau, A.A. Balandin, The effect of substrates on the Raman spectrum of graphene: Graphene-on-sapphire and graphene-on-glass, Appl Phys Lett, 91(2007)201904.

[17] W. Jie, Y.Y. Hui, Y. Zhang, S.P. Lau, J. Hao, Effects of controllable biaxial strain on the Raman spectra of monolayer graphene prepared by chemical vapor deposition, Appl Phys Lett, 102(2013)223112.

[18] A.C. Ferrari, J.C. Meyer, V. Scardaci, C. Casiraghi, M. Lazzeri, F. Mauri, S. Piscanec, D. Jiang, K.S. Novoselov, Raman spectrum of graphene and graphene layers, Phys Rev Lett, 97(2006)187401.

[19] M.A. Bissett, W. Izumida, R. Saito, H. Ago, Effect of domain boundaries on the Raman spectra of mechanically strained graphene, ACS Nano, 6(2012)10229–10238.

[20] L.B. Gao, W.C. Ren, H.L. Xu, L. Jin, Z.X. Wang, L.P. Ma , Z.Y. Zhang, Q. Fu, L.M. Peng, X.H. Bao, H.M. Cheng, Repeated growth and bubbling transfer of graphene with millimetre-size single-crystal grains using platinum, Nat Commun, 6(2012)699.

[21] J.M. Caridad, F. Rossella, V. Bellani, M. Maicas, M. Patrini, E. Díez, Effects of particle contamination and substrate interaction on the Raman response of unintentionally doped graphene, J Appl Phys, 108(2010)084321.

RSC Advances Accepted Manuscript

[22] Q. Wang, R. Hu, Y. Shao, The combined effect of surface roughness and internal stresses on nanoindentation tests of polysilicon thin films, J Appl Phys, 112(2012)044512.

[23] P. Blake, E.W. Hill, A.H. Castro Neto, Making graphene visible, Appl Phys Lett, 91(2007)063124.

[24] D.M. Basko, Erratum: Theory of resonant multiphonon Raman scattering in graphene, Phys Rev B, 78(2008)125418.

[25] T.M. Mohiuddin, A. Lombardo, R.R. Nair, A. Bonetti, G. Savini, D.M. Basko, C. Galiotis, N. Marzari, Uniaxial strain in graphene by Raman spectroscopy: G peak splitting, Grüneisen parameters, and sample orientation, Phys Rev B, 79(2009)205433.

[26] L. Gong, I.A. Kinloch, R.J. Young, I. Riaz, R. Jalil, K.S. Novoselov, Interfacial stress transfer in a graphene monolayer nanocomposite, Adv Mater, 22(2010)2694.

RSC Advances Accepted Manuscript

Figure captions

FIG. 1. (a) SEM image of the patterned substrate. (b) Graphene covering substrate characterized by AFM combined with confocal laser microscopy. Below is the section analysis of sample, which can offer detailed information about sample height; (c) confocal laser microscopy and (d) SEM images of graphene covering substrate.

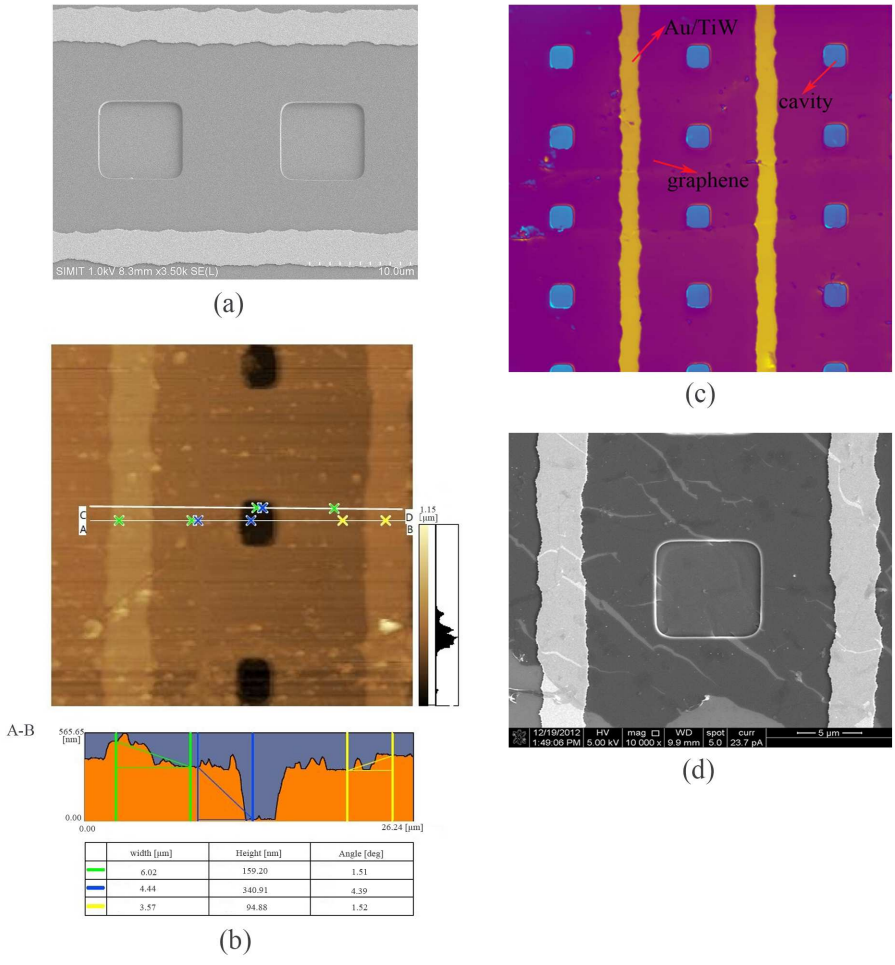

RSC Advances Accepted Manuscript

FIG. 2. AFM analyses of surface roughness of 300-nm-thick SiO_2 layer and cavity, respectively. (a) and (c) AFM images of sample; (b) and (d) section analyses of surface roughness.

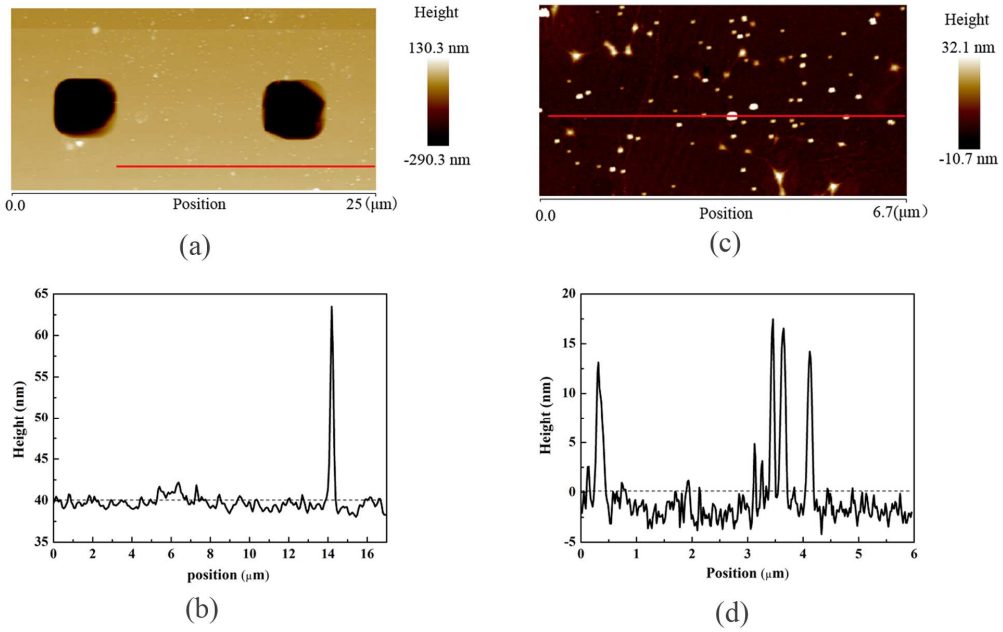

RSC Advances Accepted Manuscript

FIG. 3. (a) and (b) 3D images of sample morphology.

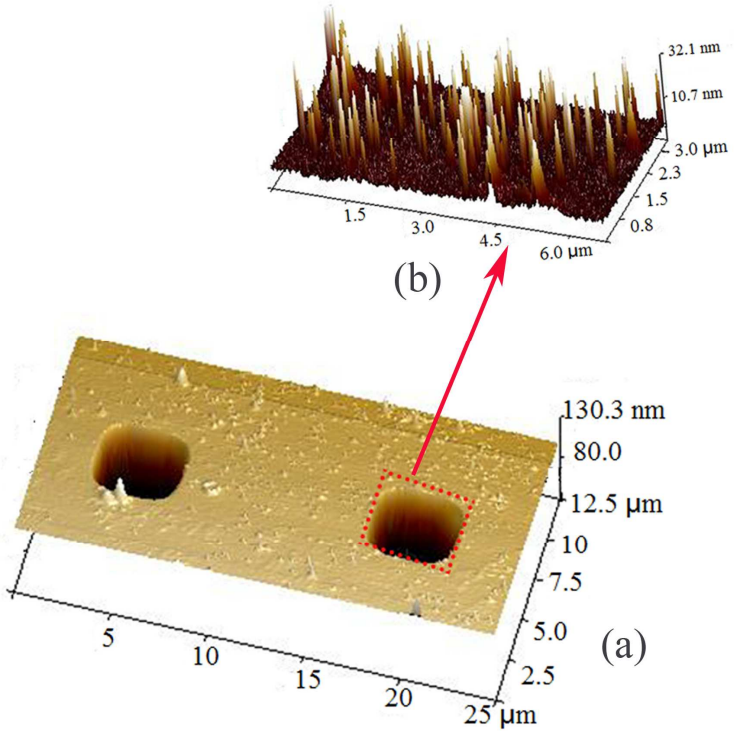

RSC Advances Accepted Manuscript

FIG. 4. Raman analysis of graphene located in the area shown in Fig. 1(d). (a) Raman spectra of graphene; (b) differences in 2D band of Raman spectra; (c) Lorentz fitting of 2D band of graphene covering 300-nm-thick SiO_2 layer; (d) Lorentz fitting of 2D band of graphene covering cavity; (e) Raman map of G peak intensity; (f) Raman map of FWHM of 2D peak; (g) Raman map of 2D peak frequency (ω_{2D}).

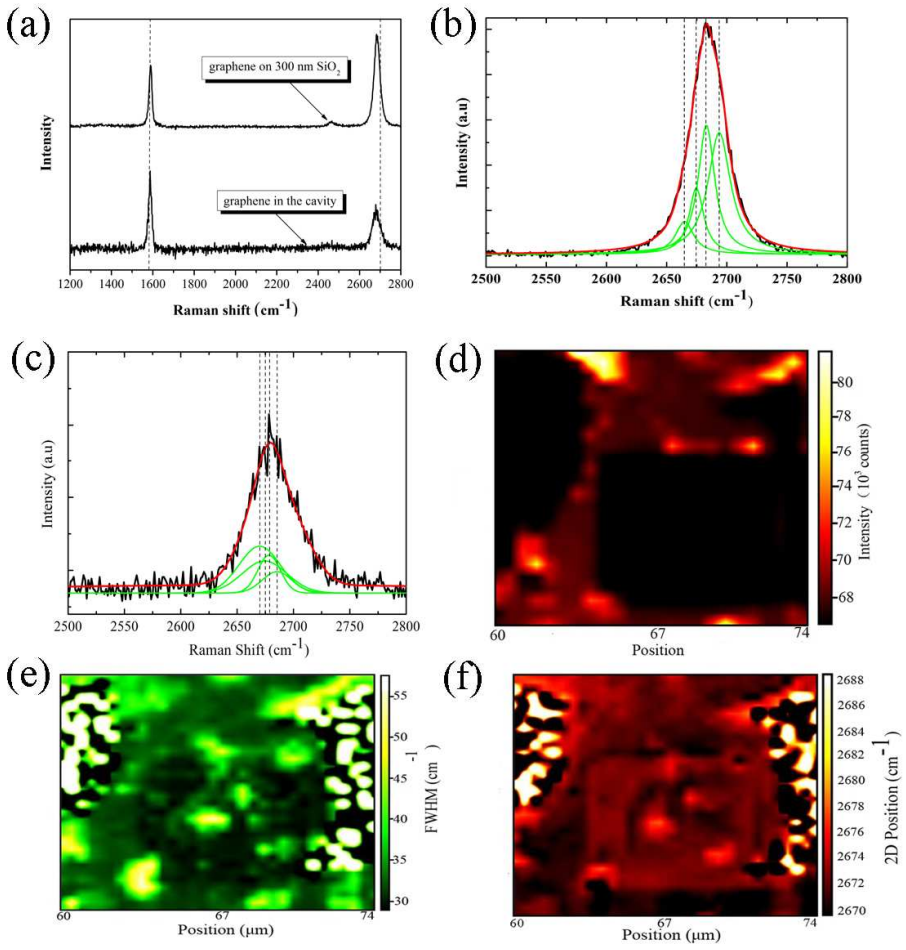

RSC Advances Accepted Manuscript

FIG. 5. 2D peak and mechanical strain distribution along the position on the substrate. Red line represents 2D peak frequency; black line represents strain distribution.

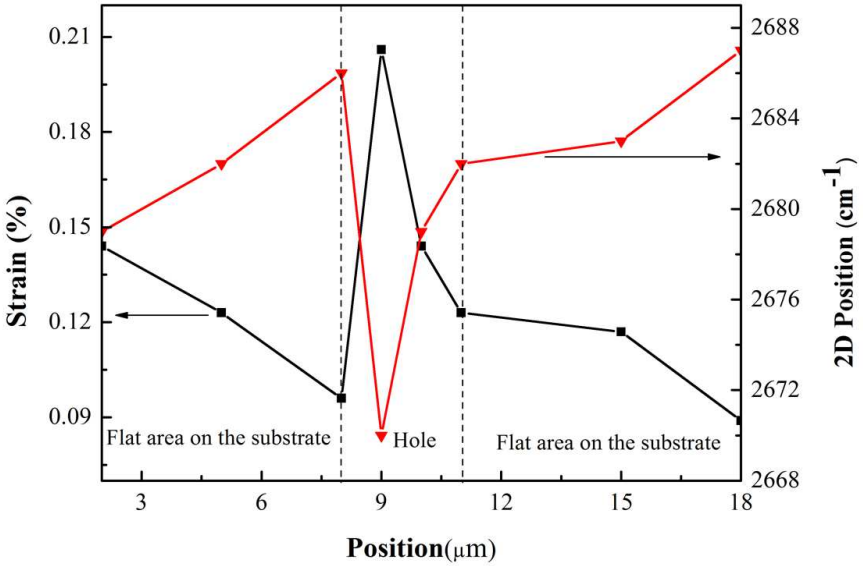

RSC Advances Accepted Manuscript

FIG. 6. Relationship between *dStrain / dX* **and position.**

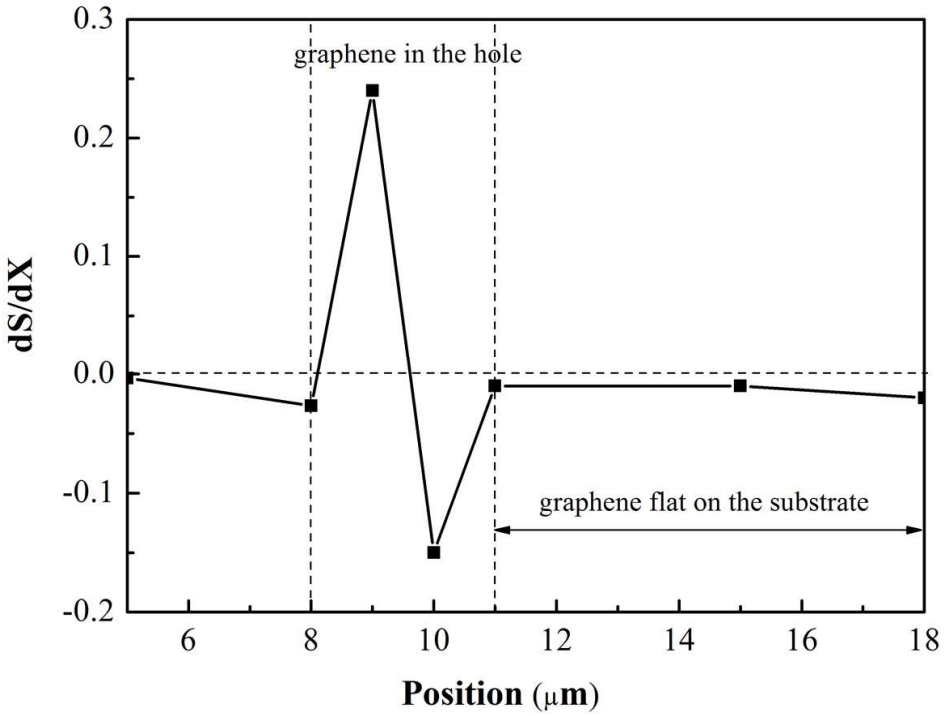

RSC Advances Accepted Manuscript